

# On Turbulent Flow Near a Wall

E. R. VAN DRIEST\*

*North American Aviation, Inc.*

## SUMMARY

A theory which provides a continuous velocity and shear distribution for turbulent flow near a smooth wall is developed. The analysis also forms the basis for the theoretical calculation of the velocity profiles and resistance owing to roughness or vortex generation. The theory checks well with experimental data.

## SYMBOLS

$y$	= distance from wall
$a$	= pipe radius
$D$	= pipe diameter
$\bar{u}$	= mean local velocity parallel to wall
$u', v'$	= velocity fluctuations parallel and normal to flow
$\rho$	= mass density
$\mu$	= coefficient of viscosity
$\tau$	= shear stress
$r$	= velocity correlation coefficient
$l$	= mixing length
$K$	= universal constant in $l = Ky$
$\kappa$	= modified universal constant
$\epsilon$	= eddy viscosity
$k$	= size of roughness
$f$	= friction factor = $8\tau_w/\rho V^2$
$V$	= average section velocity
$R$	= Reynolds Number = $VD/\nu$
$\nu$	= kinematic viscosity
$w$	= subscript denoting wall
$t$	= subscript denoting turbulence
<i>turb</i>	= subscript denoting turbulence
<i>max</i>	= subscript denoting maximum
$u_*$	= $\bar{u}/\sqrt{\tau_w/\rho}$
$y_*$	= $\sqrt{\tau_w/\rho} \cdot y/\nu$
$l_*$	= $\sqrt{\tau_w/\rho} \cdot l/\nu$
$k_*$	= $\sqrt{\tau_w/\rho} \cdot k/\nu$
$a_*$	= $\sqrt{\tau_w/\rho} \cdot a/\nu$
$A_*$	= constant

## INTRODUCTION

THE PURPOSE of this report is to present an analysis which will yield a continuous velocity and shear distribution for turbulent flow near a smooth wall. The results of such an analysis should be particularly useful in the study of convective heat transfer by liquids over a wide range of Prandtl Number. The report pertains to incompressible fluids only.

It is found that the theory fits the measured velocity-profile data for smooth walls. The analysis also leads to the theoretical calculation of velocity profiles and friction factors for rough pipes and/or vortex generators.

## ANALYSIS

When the Navier-Stokes equations are written in terms of mean velocities and fluctuations from the

Presented at the 1955 Heat Transfer and Fluid Mechanics Institute, Los Angeles, June 23-25, 1955. Received October 6, 1955.

\* Staff Specialist, Missile Development Division.

mean and then averaged with respect to time, rearrangement of the resulting equation allows the total shear stress  $\tau$  to be identified as

$$\tau = \mu(\partial\bar{u}/\partial y) - \overline{\rho u'v'} \quad (1)$$

where  $\bar{u}$  is the mean velocity parallel to the wall,  $u'$  the instantaneous fluctuation of velocity in the direction of  $\bar{u}$ ,  $v'$  the cross fluctuation of velocity in the direction normal to the wall,  $y$  the length scale normal to the wall and measured positive from the wall,  $\rho$  the density of the fluid, and  $\mu$  the coefficient of viscosity of the fluid. The first term on the right-hand side of Eq. (1) represents the effect of viscosity on the mean flow whereas the second term is the Reynolds stress. In turbulent flow away from a wall, the Reynolds stress is of considerably greater magnitude than the viscous stress; however, the more a smooth wall is approached, the greater becomes the role of the viscous stress until finally, at the wall, viscosity predominates.

The viscous effect of the proximity of the wall may be estimated in the following manner:

Consider an infinite flat plate undergoing simple harmonic oscillation parallel to the plate in an infinite fluid. As was shown by Stokes,<sup>1</sup> the amplitude of the motion diminishes from the wall as a consequence of the factor  $\exp(-y/A)$  where  $A$  is a constant depending upon the frequency of oscillation of the plate and the kinematic viscosity  $\nu$  of the fluid. Hence, when the plate is fixed and the fluid oscillates relative to the plate, the factor  $[1 - \exp(-y/A)]$  must be applied to the fluid oscillation to obtain the damping effect on the wall. Now, according to Prandtl, the total shear stress for turbulent flow is written as

$$\tau = \mu(\partial\bar{u}/\partial y) + \rho r \sqrt{u'^2} \cdot \sqrt{v'^2} \quad (2)$$

where  $r$  is the correlation coefficient defined by  $\overline{u'v'} = -r\sqrt{u'^2} \cdot \sqrt{v'^2}$ . Introduction of the mixing lengths  $l_1$  and  $l_2$  defined by  $\sqrt{u'^2} = l_1 \partial\bar{u}/\partial y$  and  $\sqrt{v'^2} = l_2 \partial\bar{u}/\partial y$ , respectively, then gives

$$\tau = \mu(\partial\bar{u}/\partial y) + \rho r l_1 l_2 (\partial\bar{u}/\partial y)^2 \quad (3)$$

The quantity  $r l_1 l_2$  is finally lumped into one overall length  $l$  to yield

$$\tau = \mu(\partial\bar{u}/\partial y) + \rho l^2 (\partial\bar{u}/\partial y)^2 \quad (4)$$

Furthermore, when it is assumed that  $l = Ky$ , where  $K$  is called the universal mixing constant, Eq. (4) becomes

$$\tau = \mu(\partial\bar{u}/\partial y) + \rho K^2 y^2 (\partial\bar{u}/\partial y)^2 \quad (5)$$

which is supposed to represent mean fully developed turbulent flow near a wall. However, such fully

developed turbulent motion occurs only beyond a distance sufficiently remote from the wall that the very eddies themselves are not damped in turn by the nearness of the wall. Indeed, near a wall, the damping factor would be  $[1 - \exp(-y/A)]$  for each mean velocity fluctuation in Eq. (2), and hence Eq. (5) should be modified to become

$$\tau = \mu(\partial\bar{u}/\partial y) + \rho K^2 y^2 [1 - \exp(-y/A)]^2 (\partial\bar{u}/\partial y)^2 \quad (6)$$

in order to take into account the mean motion all the way to a smooth wall.

One could argue that the presence of the wall modifies the universal constant so that

$$\kappa = K[1 - \exp(-y/A)] \quad (7)$$

or that the mixing length must be changed to

$$l = Ky[1 - \exp(-y/A)] \quad (8)$$

It is convenient to write Eq. (6) in dimensionless form. Thus, putting

$$u_* = \bar{u}/\sqrt{\tau_w/\rho} \quad y_* = \sqrt{\tau_w/\rho} \cdot y/\nu \quad (9)$$

where  $\tau_w$  is the shear at the wall, Eq. (6) becomes

$$\tau/\tau_w = (\partial u_*/\partial y_*) + K^2 y_*^2 [1 - \exp(-y_*/A_*)]^2 \times (\partial u_*/\partial y_*)^2 \quad (10)$$

in which  $A_*$  is a constant of the turbulence. Furthermore,

$$\kappa = K[1 - \exp(-y_*/A_*)] \quad (11)$$

$$l_* = Ky_*[1 - \exp(-y_*/A_*)] \quad (12)$$

where  $l_* = \sqrt{\tau_w/\rho} \cdot l/\nu$ .

According to Eq. (1), the Reynolds stress  $\tau_t$  is obtained from

$$\tau = \mu(\partial\bar{u}/\partial y) + \tau_t \quad (13)$$

in which  $\tau_t = -\rho\overline{u'v'}$ . Hence, with Eq. (9),

$$\tau_t = \tau - \tau_w(\partial u_*/\partial y_*) \quad (14)$$

$$\text{whence} \quad \tau_t/\tau_w = (\tau/\tau_w) - (\partial u_*/\partial y_*) \quad (15)$$

The eddy viscosity  $\epsilon$  is obtained from

$$\tau = \mu(\partial\bar{u}/\partial y) + \epsilon(\partial\bar{u}/\partial y) = (\mu + \epsilon)(\tau_w/\mu) \cdot (\partial u_*/\partial y_*) \quad (16)$$

$$\text{so that} \quad \epsilon/\mu = [(\tau/\tau_w)/(\partial u_*/\partial y_*)] - 1 \quad (17)$$

**Smooth Wall**

For boundary-layer flow with zero pressure gradient,  $\partial\tau/\partial y = 0$  at the wall and therefore  $\tau \approx \tau_w$  near the wall. Hence, Eq. (10) yields

$$\frac{\partial u_*}{\partial y_*} = \frac{2}{1 + \sqrt{1 + 4K^2 y_*^2 [1 - \exp(-y_*/A_*)]^2}} \quad (18)$$

whereupon

$$u_* = \int_0^{y_*} \frac{2dy_*}{1 + \sqrt{1 + 4K^2 y_*^2 [1 - \exp(-y_*/A_*)]^2}} \quad (19)$$

Then, from Eqs. (15) and (17), respectively,

$$\tau_t/\tau_w = 1 - (\partial u_*/\partial y_*) \quad (20)$$

$$\epsilon/\mu = [1/(\partial u_*/\partial y_*)] - 1 \quad (21)$$

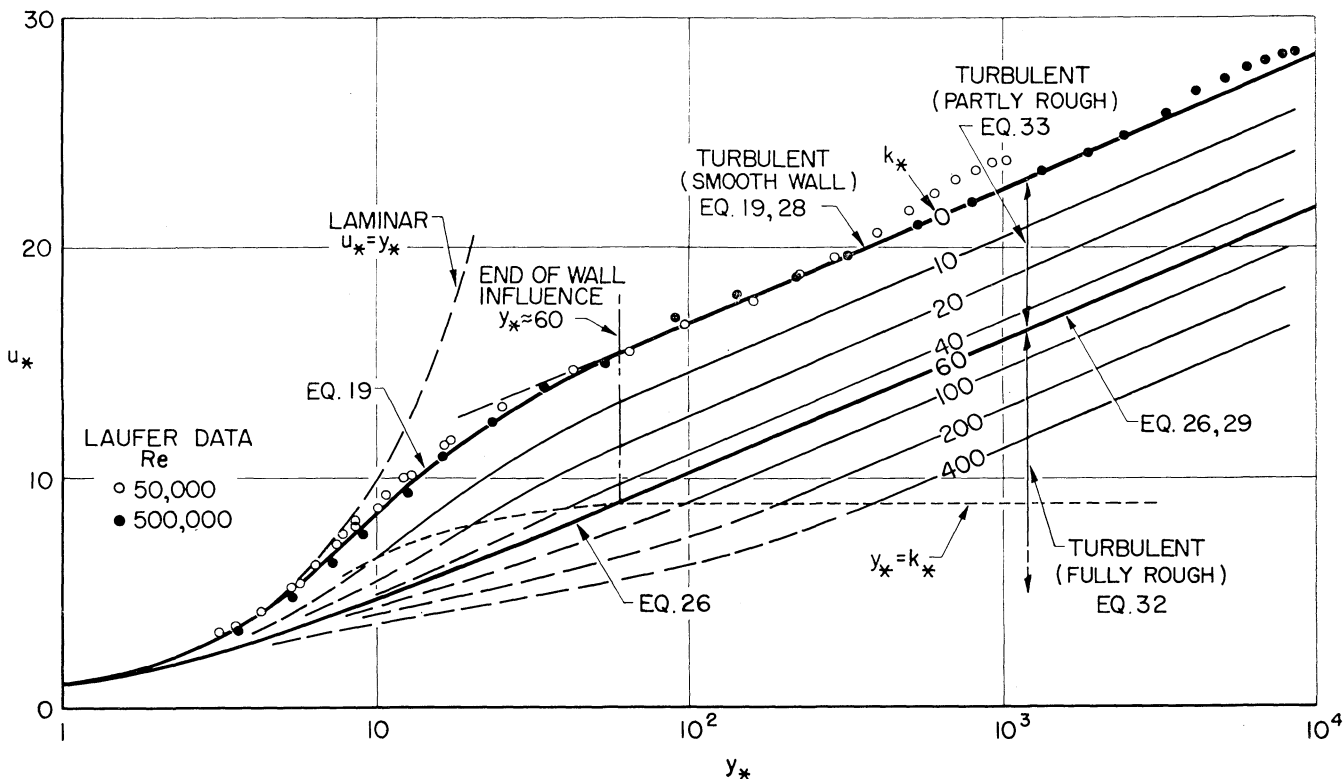


FIG. 1. Semilogarithmic plot of velocity profiles for turbulent flow near smooth and rough walls. Comparison of theory and experiment for a smooth pipe.

For large  $y_*$ , Eq. (19) becomes

$$u_* = \text{const.} + (1/K) \ln y_* \tag{22}$$

which is the von Kármán law for fully turbulent flow—i.e., where viscosity does not affect even the mean flow.

The above analysis applies to a smooth wall under which condition the proximity of the wall has a stabilizing effect upon the eddies owing to viscosity. Of course, the opposite could be argued—namely, that the wall loses its control of the fluid elements with distance from the wall according to the same law.

**Rough Wall (Vortex Generation)**

The stabilizing effect of the wall can, however, be nullified by introducing an artificial mixer at the wall—viz., roughness. When sufficient roughness is introduced to stir up the motion near the wall (vortex generation), the factor  $\exp(-y_*/A_*)$  should disappear from the above equations so that Eqs. (11), (12), and (19) should become, respectively,

$$\kappa = K \tag{23}$$

$$l_* = Ky_* \tag{24}$$

$$\partial u_*/\partial y_* = 2/[1 + \sqrt{1 + (2Ky_*)^2}] \tag{25}$$

which integrates to

$$u_* = \frac{1}{K} \left\{ \frac{1 - \sqrt{1 + (2Ky_*)^2}}{2Ky_*} + \ln \left[ 2Ky_* + \sqrt{1 + (2Ky_*)^2} \right] \right\} \tag{26}$$

For large  $y_*$ , Eq. (26) becomes

$$u_* = \text{const.} + (1/K) \ln y_*$$

which is again the von Kármán law for fully developed turbulent flow.

It is expected that Eq. (26) should represent the beginning of fully turbulent flow clear to the wall—i.e., flow which feels only the effect of viscosity on the mean motion and not a viscous effect of the nearness of the wall on the individual eddies.

The above results for flow in the vicinity of both smooth and rough walls are also approximately valid with a pressure gradient in the direction of the flow because the shear stress near the wall is approximately equal to the wall stress.

COMPARISON WITH EXPERIMENT

**Velocity Profiles**

Fig. 1 shows a semilogarithmic plot of the mean-velocity data obtained by Laufer<sup>2</sup> for fully developed turbulent flow in a smooth pipe at two Reynolds Numbers—namely 50,000 and 500,000—based on the diameter of the pipe. Also plotted in the figure is Eq. (19) when  $K = 0.4$  and  $A_* = 26$ . It appears that the theory follows the data quite well.

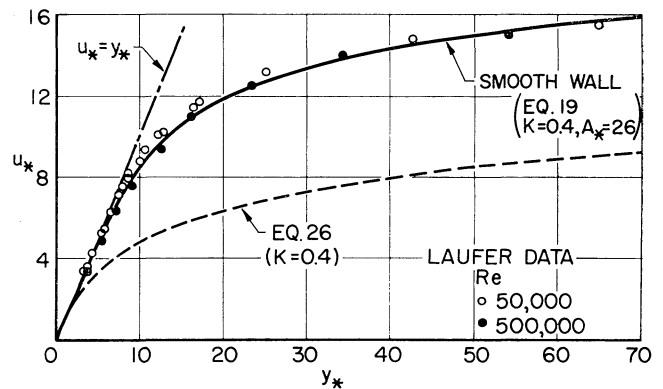


FIG. 2. Comparison of theory and experiment for turbulent flow near the wall of a smooth pipe.

For a smooth wall, the asymptotic curves at the wall and out in the so-called fully developed turbulent flow are, respectively,

$$u_* = y_* \tag{27}$$

$$u_* = 5.24 + 5.75 \log_{10} y_* \tag{28}$$

Fig. 2 is a Cartesian-coordinate plot of the Laufer data and Eq. (19) for the range  $y_* < 70$ .

It should be mentioned here that, in order to fit Eq. (19) to Nikuradse's smooth-wall data,<sup>3</sup> it would be necessary that  $A_* = 27$ .

The velocity profile for the beginning of complete roughness, Eq. (26), is plotted in Fig. 1 with  $K = 0.4$ . The asymptote in the stream is

$$u_* = -1.325 + 5.75 \log_{10} y_* \tag{29}$$

Eq. (26) is plotted also in Fig. 2. Of particular interest is the fact that only one constant,  $K$ , appears in Eq. (26).

It is evident from the smooth-wall curve of Fig. 1 that the viscous damping effect of the wall extends out to about  $y_* = 60$ . Therefore, it is expected that any roughness elements should also extend to about  $y_* = 60$  before they completely nullify the viscous influence of the wall. Thus, if there are no viscosity effects for roughnesses greater than  $k_* = \sqrt{\tau_w/\rho} \times k/\nu = 60$ , where  $k$  is the average roughness size, then the general velocity profile beyond the roughness protuberances would be, from dimensional analysis,

$$u_* = \text{const.} + (1/K) \ln (y/k) \tag{30}$$

$$= \text{const.} + (1/K) \ln k_* + (1/K) \ln y_* \tag{31}$$

so that, from Eq. (29) when  $K = 0.4$  and  $k_* = 60$ ,

$$u_* = 8.95 - 5.75 \log_{10} k_* + 5.75 \log_{10} y_* \tag{32}$$

The two regions of flow, one under viscous influence of the wall and the other with a wholly rough wall, are indicated in Fig. 1. In the region of viscous influence of the wall, the roughness height  $k_*$  is less than 60—i.e., for  $k_* < 60$ , the nearness of the wall still shows some effect through viscous damping.

An estimate can be made of the velocity profile when the roughness is within the viscous influence of the wall—i.e.,  $k_* < 60$ . It was seen above that the

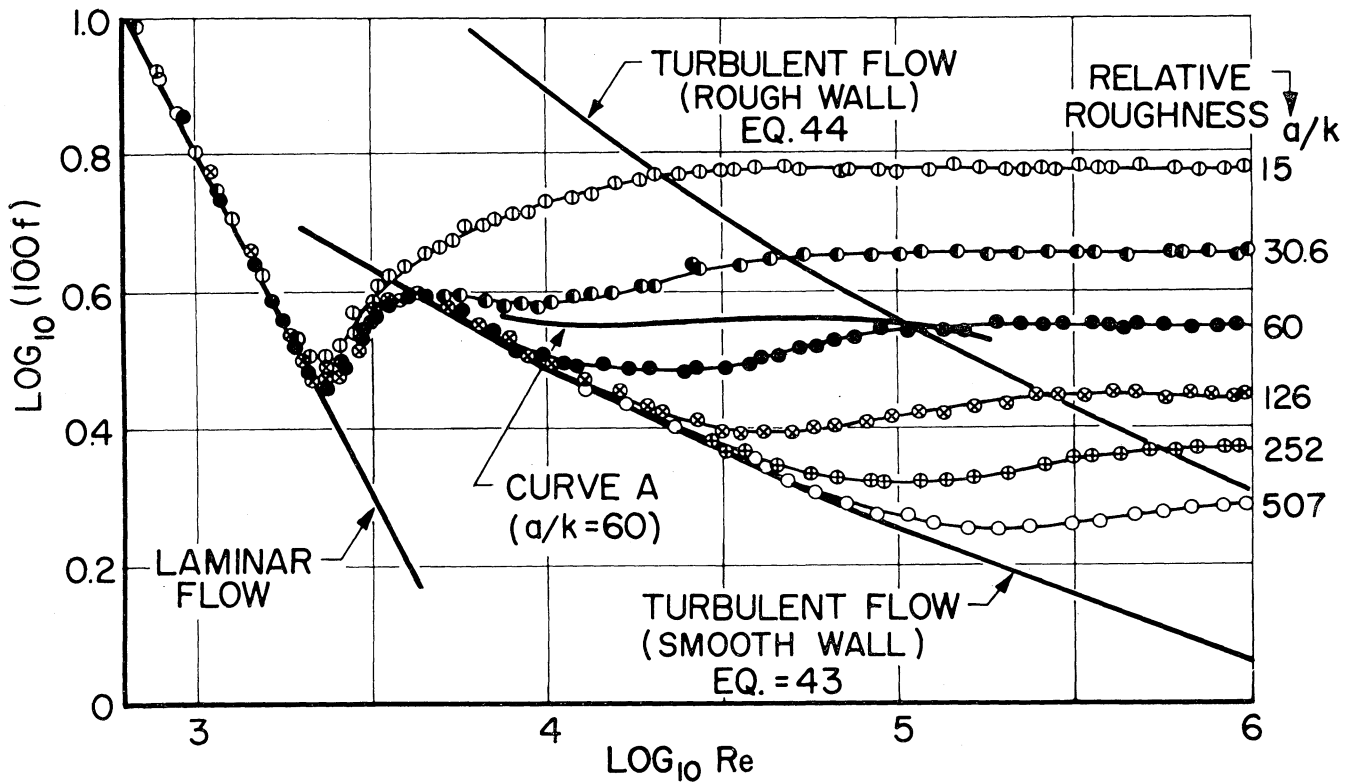


FIG. 3. Friction factor for flow in a rough pipe.

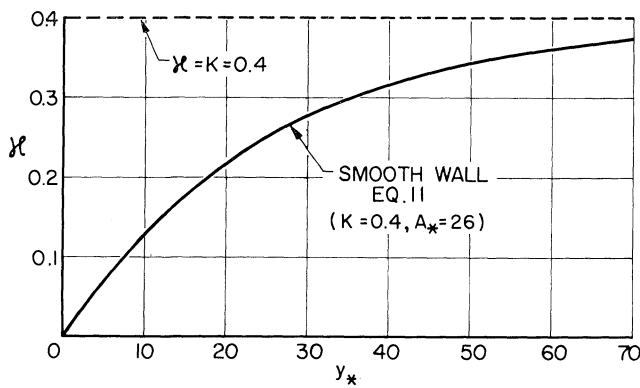


FIG. 4. Modified universal constant for turbulent flow near a smooth wall.

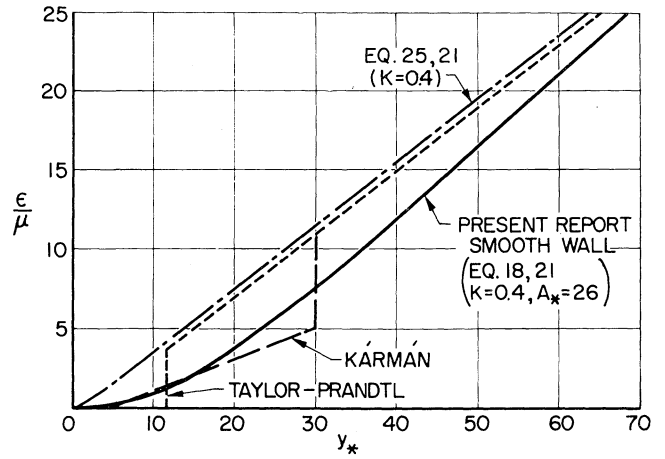


FIG. 6. Eddy-viscosity variation for flow near a smooth wall.

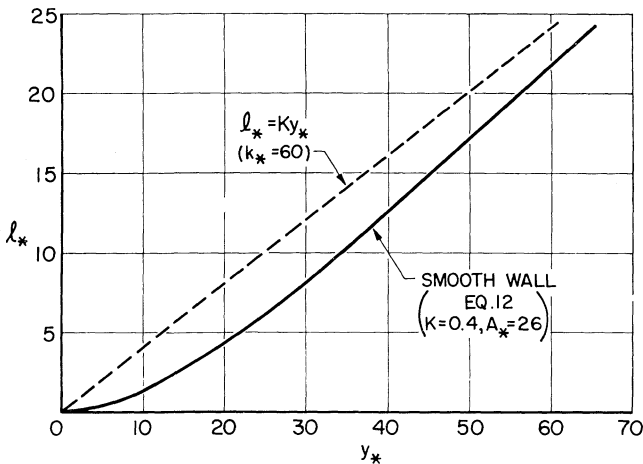


FIG. 5. Modified mixing length for turbulent flow near a smooth wall.

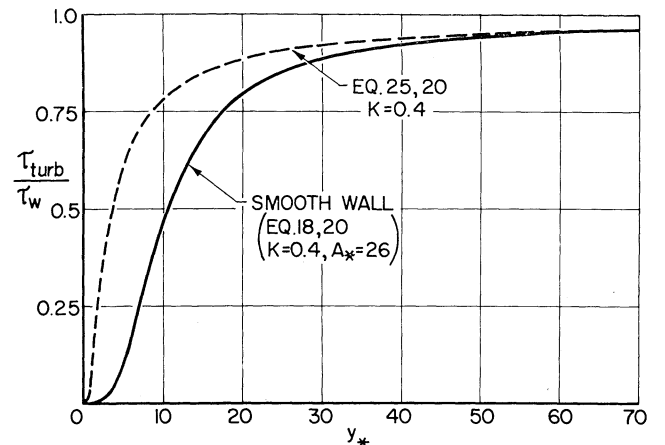


FIG. 7. Turbulent shear-stress variation for flow near a smooth wall.

beginning of the complete roughness effect was felt on the flow when the roughness protuberances projected out sufficiently far from the wall to disrupt the viscous effect of the wall. Thus, the factor  $\exp(-y_* \div A_*)$  was artificially eliminated. However, this can be expressed mathematically by adding a local vortex-generation factor  $\exp(-y_*/26)$  to the damping factor  $-\exp(-y_*/26)$ . But the vortex-generation factor should grow with the size of the roughness, and, therefore, such a factor should have the form  $\exp(-60y_*/26k_*)$  so that, at  $y_* = k_* = 60$ , the disturbance factor owing to roughness just offsets the damping factor. Obviously, as  $k_*$  changes, the roughness factor remains similar. The velocity profile including roughness then becomes

$$u_* = \int_0^{y_*} \frac{2dy_*}{1 + \sqrt{1 + 4K^2y_*^2[1 - \exp(-y_*/26) + \exp(-60y_*/26k_*)]^2}} \tag{33}$$

so that the damped universal constant and damped mixing length become, respectively,

$$\kappa = K[1 - \exp(-y_*/26) + \exp(-60y_*/26k_*)] \tag{34}$$

$$l_* = Ky_*[1 - \exp(-y_*/26) + \exp(-60y_*/26k_*)] \tag{35}$$

Some velocity profiles outside of the roughness elements are plotted in Fig. 1. It is seen that the smooth wall results when  $k_* = 0$ . On the other hand, if Eq. (32) is assumed to hold for all sizes of roughness, then it will be found that, for smooth effects, it is not necessary that  $k_* = 0$  but rather that  $k_* = 4$  because, from Eqs. (28) and (32),

$$5.24 = 8.95 - 5.75 \log_{10} k_*$$

whence  $k_* = 4$ . It seems more logical, however, that  $k_* = 0$  rather than  $k_* = 4$  represents a smooth wall.

**Friction Factor**

It is readily shown that the mean and maximum velocities of the semilogarithmic profile are related by

$$(u_{max} - V)/\sqrt{\tau_w/\rho} = (3/2K) = 3.75 \tag{36}$$

where  $V$  is the average section velocity and  $K = 0.4$ . Also, the friction factor  $f$  for pipes is given by

$$f = 8\tau_w/\rho V^2 \tag{37}$$

Hence, from Eqs. (28)—with  $y = a$ , (36), and (37), there results for a smooth wall

$$\sqrt{8/f} = 1.49 + 5.75 \log_{10} [\sqrt{\tau_w/\rho} \cdot (a/\nu)] \tag{38}$$

$$= 1.49 + 5.75 \log_{10} [\sqrt{f/a} \cdot (V/2) \cdot (D/\nu)] \tag{39}$$

$$= 1.49 + 5.75 \log_{10} (1/4\sqrt{2}) + 5.75 \log_{10} (R\sqrt{f}) \tag{40}$$

$$= -2.84 + 5.75 \log_{10} (R\sqrt{f}) \tag{41}$$

in which  $D = 2a$  and  $R = VD/\nu$ . Hence, upon division by  $\sqrt{8}$ , the friction law for a smooth wall becomes

$$1/\sqrt{f} = -1.0 + 2.04 \log_{10} (R\sqrt{f}) \tag{42}$$

However, the test data of Nikuradse<sup>3</sup> indicate that the constants should be adjusted so that

$$1/\sqrt{f} = -0.8 + 2 \log_{10} (R\sqrt{f}) \tag{43}$$

For the beginning of complete roughness, Eq. (29) gives

$$1/\sqrt{f} = -3.3 + 2 \log_{10} (R\sqrt{f}) \tag{44}$$

Eqs. (43) and (44) are plotted in Fig. 3 along with curves faired through the rough-wall data of Nikuradse.<sup>4</sup>

It is seen that the semitheoretical formula, Eq. (44), crosses all roughness curves at approximately the end of transition for each relative roughness. This result is particularly interesting because only one constant,  $K$ , entered in the derivation of Eq. (44). Thus, the concept of generation of vortices by roughness appears justified.

The general formula for complete roughness (independency with Reynolds Number) is now deducible from Eqs. (32), (36), and (37), whence

$$\sqrt{8/f} = 5.15 - 5.75 \log_{10} k_* + 5.75 \log_{10} a_* \tag{45}$$

where  $a_* = \sqrt{\tau_w/\rho} a/\nu$ . Division by  $\sqrt{8}$  gives

$$1/\sqrt{f} = 1.82 - 2.04 \log_{10} (a_*/k_*) \tag{46}$$

which agrees well with the experimental formula—viz.,

$$1/\sqrt{f} = 1.74 - 2 \log_{10} (a_*/k_*) \tag{47}$$

representing the horizontal relative roughness lines in Fig. 3. It is noted that the only constant necessary to be evaluated experimentally in the derivation of Eq. (46) was  $K$  in  $l = Ky$ .

It is also possible to estimate theoretically the friction curves in the transition region of Fig. 3—i.e., curves of various relative roughness connecting the curves of Eqs. (43) and (44). Thus, one such curve, curve A, is obtained for  $a/K = 60$  through use of Eqs. (33), (36), and (37) with arbitrary  $k_*$  and the relation

$$R\sqrt{f} = 4\sqrt{2} \cdot k_* \cdot (a/k) \tag{48}$$

Curve A has the proper trend.

**Other Properties Near a Wall**

Figs. 4 and 5 show the distributions of the damped universal constant and of the damped mixing length according to Eqs. (34) and (35), respectively, for  $K = 0.4$ .

Fig. 6 gives the corresponding eddy viscosity according to Eq. (21) for  $\tau = \tau_w$ . Also plotted in Fig. 6 are the assumptions of Taylor<sup>5</sup> and Prandtl,<sup>6</sup> and of von Kármán.<sup>7</sup> The shear distribution, Eq. (20), is shown in Fig. 7. Direct measurements of the cross correlation  $\overline{u'v'}$  are apparently not available for  $y_*$  less than about 100.

(Continued on page 1036)

Downloaded by UNIVERSITY OF ILLINOIS on March 14, 2015 | http://arc.aiaa.org | DOI: 10.2514/6.8.3713

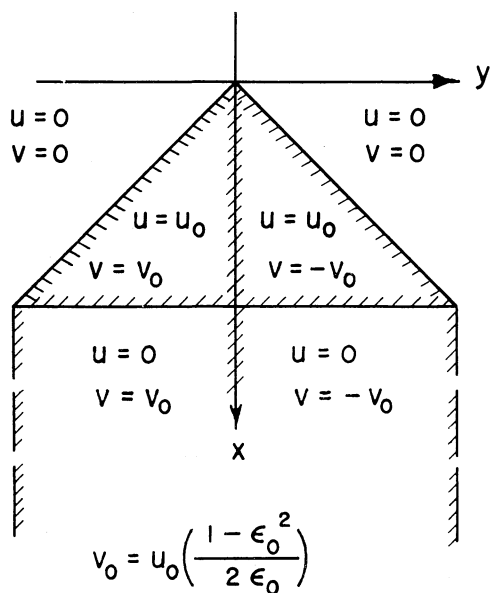


FIG. 15. Constant pressure delta wing.

a highly cambered one and is characterized by logarithmic infinities in slope at the leading and trailing edges and along the centerline.

The reverse-delta constant pressure wing is obtained by the superposition

$$G_8(x, y, z; \epsilon_0, c) = -(1/2)G_6(x, y + b, z; \epsilon_0, c) + (1/2)G_6(x, y - b, z; -\epsilon_0, c) - \epsilon_0 G_5(x, y, z; 1, c)$$

where  $b$  is given in Eq. (11). This field is indicated in Fig. 16.

Since any polygonal plan form which does not have streamwise tips (parallel to the  $x$  axis) and which is symmetric about a streamwise axis can be partitioned into isosceles triangles like those of Figs. 15 and 16, these fields may be combined to obtain a constant pressure wing of such a plan form. In such a superposition, the singularities in downwash in the component flows will cancel except on the boundaries of and downstream of the vertices of the resultant wing.

CONCLUDING REMARKS

The foregoing represents a very convenient method of treating polygonal source sheets and constant pres-

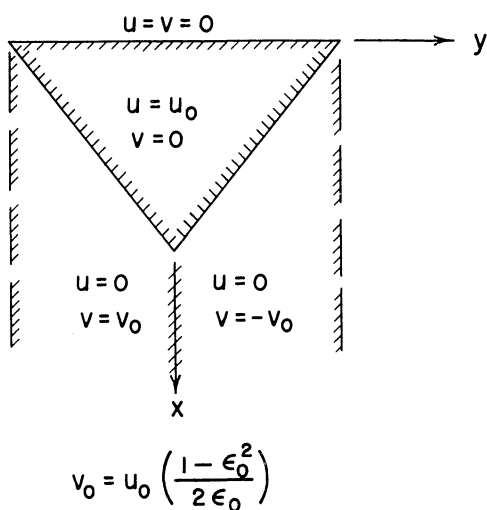


FIG. 16. Constant pressure reverse delta wing.

sure regions in potential flow. The Prandtl-Glauert transformation may be used to extend this treatment to subsonic compressible fields.

In addition it would appear that the constant pressure delta wings might be superposed to provide an approximate model for the general lifting wing. Preliminary attempts to construct such a model, using a scheme similar to the horseshoe vortex superposition of Falkner,<sup>4</sup> were not successful. The difficulties encountered appeared to be chiefly due to the presence of singularities in downwash associated with the edges of the triangular vorticity patches and the lack of a rational basis for locating downwash control points. Work in this direction is being continued.

REFERENCES

<sup>1</sup> Donkin, W. F., *Phil. Trans.* 1857. Referred to on p. 357 of Bateman, H., *Partial Differential Equations of Mathematical Physics*, Dover Publications, New York, 1944.  
<sup>2</sup> Jones, R. T., *Subsonic Flow over Thin Oblique Airfoils at Zero Lift*, NACA TN 1340, 1947.  
<sup>3</sup> Lampert, Seymour, *Conical Flow Methods Applied to Uniformly Loaded Wings in Subsonic Flow*, *Journal of the Aeronautical Sciences*, Vol. 18, No. 2, p. 107, February, 1951.  
<sup>4</sup> Falkner, V. M., *The Solution of Lifting Plane Problems by Vortex Lattice Theory*, Aero. Research Council, R&M No. 2591, 1953.

On Turbulent Flow Near a Wall

(Continued from page 1011)

REFERENCES

<sup>1</sup> Stokes, G. G., *On the Effect of the Internal Friction of Fluids on the Motion of Pendulums*, *Trans. Cambridge Philos. Soc.*, Vol. 9, 1851.  
<sup>2</sup> Laufer, John, *The Structure of Turbulence in Fully Developed Pipe Flow*, NACA TN 2954, June, 1953.  
<sup>3</sup> Nikuradse, J., *Gesetzmässigkeiten der Turbulenten Strömung in Glatten Rohren*, VDI, *Forschungsheft* 356, 1932.

<sup>4</sup> Nikuradse, J., *Strömungsgesetze in rauhen Rohren*, VDI, *Forschungsheft* 361, 1933.  
<sup>5</sup> Taylor, G. I., *Conditions at the Surface of a Hot Body Exposed to the Wind*, *Tech. Rep.*, Advisory Committee for Aeronautics, Vol. 2, R&M 272, May, 1916.  
<sup>6</sup> Prandtl, L., *Bemerkung über den Wärmeübergang im Rohr*, *Physik. Zeitschr.*, Vol. 29, 1928.  
<sup>7</sup> von Kármán, Th., *The Analogy Between Fluid Friction and Heat Transfer*, *Trans. ASME*, Vol. 61, 1939.

Downloaded by UNIVERSITY OF ILLINOIS on March 14, 2015 | http://arc.aiaa.org | DOI: 10.2514/6.3713